

Micro Hot-Embossing of Serpentine Channels on PMMA based Microfluidic devices

Yugandhar Arcot, G.L.Samuel* and Lingxue Kong^a

Manufacturing Engineering Section, Department of Mechanical Engineering
Indian Institute of Technology, Chennai - 600 036, INDIA

^aInstitute for Frontier Materials, Deakin University, Geelong, VIC-3216, AUSTRALIA

Abstract

Particle inertial focusing is a prospective technique for separation of particles using microfluidic devices. Serpentine Channels are a big potential to Particle Inertial focusing mechanism, owing to the capability of Parallelization compared to Spiral channels. The devices for inertial focusing consist of different features like Pillars, Channels and reservoirs where the features are ranging from microns to Macro scale. Hot embossing is a low cost, high production and an established method for fabrication of Microfluidic Devices. This paper demonstrates the Micro Hot-embossing process on Polymethylmethacrylate (PMMA) sheets with the above feature sizes. Nickel (Ni) master is used for embossing and is fabricated using SU-8 Photolithography and Electroforming techniques. As the devices contain macro-features, the key parameters of Hot-embossing in this study which include Temperature and Pressure are chosen accordingly. This paper studies on the effect of parameters for Geometric Fidelity and Surface roughness evaluated after Embossing of geometrical features on a PMMA sheet. The Optimal processing conditions for PMMA devices are 20°C above glass transition, with an embossing load of 35kN.

Keywords: Hot-embossing, PMMA, Serpentine Microfluidic channels, Micro and Macro-features

1. INTRODUCTION

Microfluidic devices offer a revolutionary change in increasing the ability to manipulate the particles in the Micro and Nano regime for Chemical and biological analysis in the form of Lab-on-chip devices. To fabricates microfluidic devices, Polymeric materials like Polymethylmethacrylate (PMMA) is appropriate and have been consistently used in laboratories, proved to be easily disposable, likely to have less sample contamination, and suitable for mass production [1]. Replication procedures like Hot-embossing is used in various fields to fabricate macro and micro features on polymers like PMMA [2].

Various microfluidic devices have been developed for separation of blood cells from plasma using Blood flow [3], DNA amplification [4], Cancer cells from normal cells [5] and Size based sorting of particles [6] etc. Separation of particles in Microfluidic devices is a prominent area of research considering its range of applications in industries for Food, Chemical and Biology. Technology of Separation in these devices mainly includes Passive and Active separation techniques [7]. Passive Separation techniques like Inertial-focusing depend upon the properties of the fluid and its flow along with the geometry of the fluidic profiles. The geometry of these profiles is broadly four types: Straight, Serpentine, Spiral and Expansion-Contraction. Among these serpentine channels are considered to be more appropriate for applications like inertial focusing because of the parallelizability of the channels, additional secondary forces acting on the particles [8]. Medium to mass production of these devices is the need-of-hour and polymers can possibly be a suitable material of interest.

Mostly, these microfluidic channels are fabricated on Polydimethylsiloxane (PDMS) using Lithography techniques which are suitable for low production capabilities. These techniques are largely depend upon the life of the Silicon (Si)-wafer and an alternative mold material like Nickel (Ni) needs to be chosen for higher production needs.

Fabrication technologies like Mechanical micro-machining [9], Hot-embossing [10, 11], Laser- ablation [12], Injection molding [13] are extensively studied and employed to fabricate micron sized features both on Metals and Polymers. Earlier, PMMA based Biological sensors with 60-120µm microfluidic channels have been developed and were fabricated using Hot-embossing [14], and thus a proven technique.

Hot embossing is a replication process of imprinting the features of a Master onto the substrate which requires a choice a parameters selection which are a key for good replication fidelity of features. In this article we study one of the fabrication procedures of Nickel (Ni)-master and the effect of embossing parameters like temperature and pressure on fidelity of replicating serpentine microfluidic channels on PMMA using hot-embossing.

2. EXPERIMENTAL

The fabrication of the Microfluidic devices includes the following steps: (i) Pre-master and Master Fabrication (ii) Hot- embossing, as shown in the figure 1. The design of the channels (120, 200, 400, 1180 µm) were drawn using standard L-EDIT software and transferred onto the photo-mask.

2.1. Pre-master and master fabrication

Pre-master was fabricated on 4" Silicon (Si) wafer using SU-8 lithography. Initially the Si-wafer was treated with Oxygen plasma for 5 minutes. A primary coating of SU-8-2005 was spin coated with 4000rpm to achieve a layer thickness of 5 µm. It is baked over a hotplate for upto 95°C for 2 minutes and then cooled to room temperature. The wafer is now flooded with UV light for 20 seconds. The UV exposed wafer was now post-baked upto 95°C and then developed using SU-8 developer solution. Upon development, the wafer was again treated with Oxygen plasma for 5 minutes.

The initial layer of SU-8-2005 was used to promote adhesion for the next SU-8-2025 layer to be coated. This wafer is then

*Author to whom correspondence should be made: samuelg@iitm.ac.in

spin-coated with SU-8-2025 at 1400rpm and a layer thickness of 42µm was achieved. The wafer is soft baked at 65°C and 95°C for 3 and 10 min respectively, and was then cooled down to room temperature. The wafer is exposed to UV light for 20 sec with the Photo-mask placed on it making a soft contact on the wafer. The wafer was now post baked with the same temperatures as previously and was developed using SU-8 developer solution as a final step in premaster fabrication.

The Premaster is then sputtered for a seed layer which consists of Cr and Ni respectively for 10min. The seed layer is sputtered to promote adhesion for the Ni-electroplating further. The sputtered wafer is then plunged into the galvanic bath which was at 45°C for 6 hours. Approximately, 200µm thick Ni-master was obtained as shown in the figure 1.f and features were all spread uniformly. The Ni-master is then heated to 400°C to remove any SU-8 adhered to it. To reduce the friction and easy de-molding, the Ni-master is sealed in vacuum along with 20ml Trichloro (1H, 1H, 2H, 2H-perfluorooctyl) Silane for about 24 hours before performing the embossing experiments.

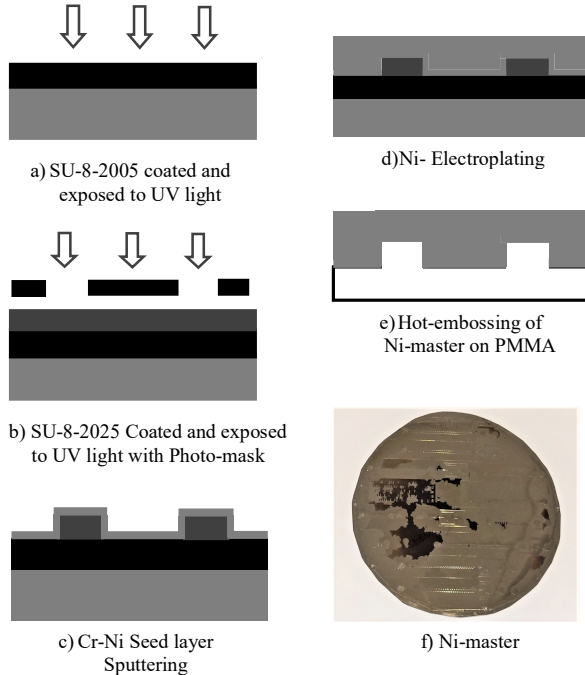


Fig. 1. Schematic of Ni-Master fabrication.

2.2. Hot-embossing

Hot embossing experiments in this study had four steps, of which, first three steps were controlled and the last step is uncontrolled: (i) Isothermal heating of the PMMA sheet with Ni-master in contact (ii) Molding of the PMMA sheet (force controlled) (iii) Cooling of the substrate, top and bottom platens, and (iv) De-molding of the substrate from the Ni-Master. In this article, the fluidic channel walls are formed by dispersing the polymer melt. The loading and temperature profiles for the hot-embossing process are as shown in the figure 2.

Hot-embosser machine, EVG 520IS, was used for performing the embossing experiments with the parameters as shown in the Table 1. Full-factorial experimental design was followed

and are performed in random. The Injection molded PMMA sheets, commercially obtained, with 1 mm thickness and 4" diameter were used for the experiments. Embossing was performed with the Ni master over the PMMA sheet. Vacuum of 0.0001mbar is maintained all through the experiment. The PMMA sheets were loaded into the embosser at room temperature. The temperature of the top and bottom platen is maintained same all over the experiments and temperature is increased with a rate of 10°C/min.

Initially a load of 500N was applied on Ni-master until both the platens reach the required temperature and then required load was applied with a slew rate of 6000N/min. Later, the applied load was maintained constant throughout the experiment. The temperatures of the platens were maintained as required upto 12 min for embossing to take place and load was released once the platens reach 70°C. The platens were cooled with a rate of 2°C/min. The assumed glass transition temperature (T_g) of PMMA sheets was 110°C and loads suitable to imprint macro-features were chosen.

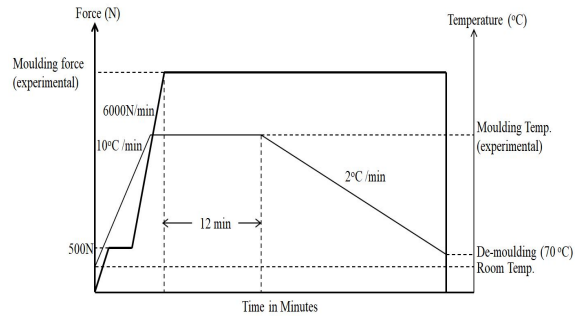


Fig. 2. Load and Temperature profiles in Hot-embossing

During molding, machine recorded a variation of +500N in load and during cooling a temperature variation of +1°C/min in top platen. After unloading the Ni-master and PMMA sheets were still in contact and few gaps were formed in between as it reached room temperature. Compressed Nitrogen gas is pumped and Isopropanol was sprayed into the gaps for complete de-molding of Ni-master and PMMA sheets and later characterized.

Table 1

Parameters used for Hot-embossing:

Sl. No.	Temperature (°C)	Load (kN)
1	T_g+10	15
2	T_g+20	25
3	T_g+30	35

2.3. Characterization of micro-channels:

All the micro-channels on the master and the PMMA sheets were characterized using Stylus and Optical Profilometer. Throughout the study, Channels were characterized at three locations across the cross-section: Channel Depth, Top and the bottom width. To eliminate the effect of fabrication defects during characterization, the channel top width and bottom width were calculated at 6 and 36 µm depths respectively and the wall angle is calculated with the vertical. Surface roughness (R_a) values were calculated in the 400 µm straight channels embossed on PMMA sheets. Readings were taken at three different places for each channel and the average values are reported in the following section.

3. RESULTS AND DISCUSSIONS:

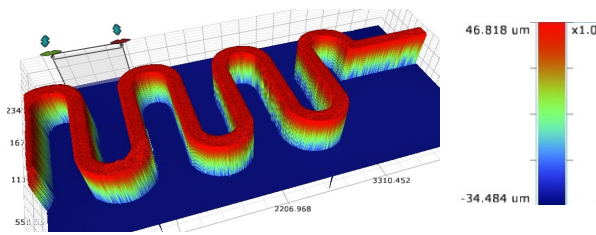
3.1. Ni-Master:

The 3D- topography and the cross sectional profile of a 200micron Channel fabricated on the Ni-master is as shown in the figure 3. The average dimensions of the channels achieved are as shown in the Table 2. For UV exposure of SU-8, the photo-mask was kept in soft contact with the wafer. The edge beads formed during spin coating were not removed from the wafer and this created a gap between wafer and the mask. Due to this gap, the polymerization of Su-8 varied and resulted in change of the dimensions than required and a trapezoidal cross section.

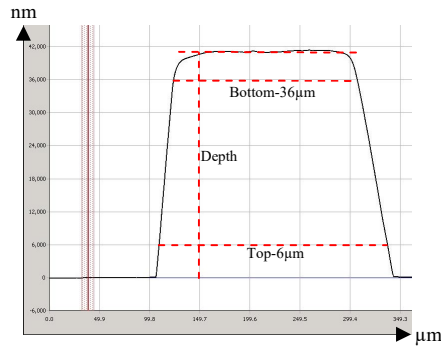
Table 2

Channel dimensions in μm on Ni-Master

Ni-Master	Bottom	Top	Depth	Angle
120	89.88	137.11	39.15	38.21
200	179.78	223.42	41.71	36.03
1180	1179.85	1223.04	41.55	35.74



a) 3D topography of 200 μm Serpentine Channel



b) Cross-sectional Profile of the Ni-master

Fig.3. 3D topography and Cross-sectional profile of Ni-Master

3.2. Effect of Temperature and load on Micro-Channels

The viscosity of the polymers decreases as the temperature increase and as the load increases the ease of the polymer flow increases. Replication accuracy should increase with the increase of temperature and load which was true at 130 $^{\circ}\text{C}$, and 140 $^{\circ}\text{C}$, as shown in the figure 4. This can be attributed to the ease of flow with higher temperature and loads, but this phenomenon was not observed at 120 $^{\circ}\text{C}$ and at any location. Also the Channel dimensions formed are smaller than the Ni-master due to recovery of the elongated polymer chains material when the load is suddenly withdrawn, which was not a cooperative phenomenon at higher loads.

During micro-hot embossing, the polymer chains may disperse or stretch to form the micro-channels. When the rate

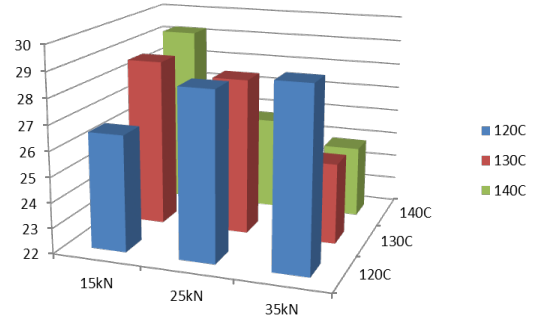


Fig.4. Effect of Load and temperature on top width of 200 μm Channel

of loading increases the material may disperse or stretch from the channel walls and recover towards the wall with time. As the flow rate will be low at temperatures close to glass transition zone, the dispersed or stretched polymer may not recover, resulting in low degree of replication at higher loads and lower temperatures. Therefore, at 120 $^{\circ}\text{C}$ as the load is increased the replication accuracy decreased, but increased at higher temperatures. It also contributes for higher recovery at 130 $^{\circ}\text{C}$, 140 $^{\circ}\text{C}$ for 35kN resulting in higher degree of replication, and the dimensions of the Channels formed are smaller than the Ni-Master.

3.3. Degree of replication with macro-features

A significant variation in change of the top width percentage from the Ni-master was observed across the dimensions (120, 200, 1180 μm) rather than locations (Top, bottom and depth). Irrespective of changes in parameters, it shows a poor degree of replication in micro-channels (38%) rather than macro-features (6%) when embossed together, as shown in the figure 5. Also the percentage of replication accuracy at top width of the channels is better compared to the bottom width. Approximate values for all the locations are shown in table 3. The diversity in the replication is due to the residual stresses developed because of high load and recovery of the material after the Ni-master was de-molded. In order to confirm the values in the table, embossing experiments were repeated at 120 $^{\circ}\text{C}$ and 15kN.

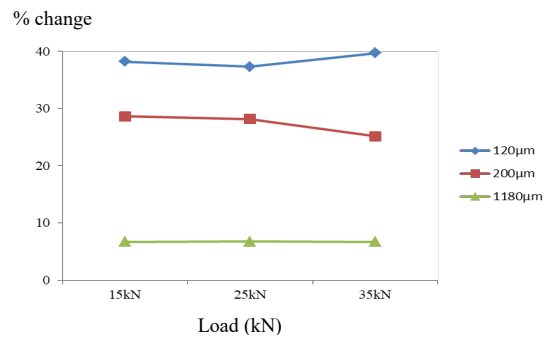


Fig. 5. Percentage of Replication accuracy of top width with varying loads at 130 $^{\circ}\text{C}$

Table 3

Percentage change in replication accuracy compared to master

	Bottom (%)	Top (%)	Depth (%)
120 μm	53.64	38.14	-1.98
200 μm	34.02	27.34	2.64
1180 μm	6.9	6.46	4.06

3.4. Roughness of Hot-embossing

Surface roughness represents the replication accuracy of embossing the fluidic channels. The deviation of the surface roughness values from the master depends upon effects like adhesion, polymer flow, experimental conditions and distortion of the surface during de-molding. This deviation shows there may be a damage or distortion on the surface which may lead to variation in dimensions and biocompatibility of embossed surfaces. The R_a values obtained from the Profilometer on Ni-master were ranging between 0.25 to 0.35 μm , and on fluidic channels were 0.15 to 0.7 μm . At 130°C and for all loads (15, 25, 35kN) the R_a values ranged between 0.25 to 0.35micron, same as of the Ni-master, and therefore showing a good replication fidelity.

3.5. Defects after embossing

Defects occurred because of the uncontrolled de-molding step, in-consistent polymer flow and sudden withdrawal of the parameters. Apart from the replication accuracy, cracks appeared consistently near the edges of the micro-channels PMMA sheet, and were absent near the Macro-features. This is due to the high concentration of the residual stresses near the Micro-features. Also, the Ni-master is not rigid like Si-wafer which may have damaged the walls and edges during de-molding. Though the top-edge of the channels on the Ni-master was not rounded, round-edges appeared on the fluidic channels further depleting the replication accuracy.

4. Conclusions

In this paper, the demonstration was focused on fabricating a Ni-master using SU-8 and imprinting the Macro and Micro features on PMMA sheets with temperature and pressure as varying parameters. Trapezoidal cross-section, Rounded edges at the bottom of the channels and adhered SU-8 appeared on the Ni-Master. The parameters chosen in this article favored for embossing the macro-features compared to the micro-channels, but at 130°C, 35kN the degree of replication was good for micro-channels too. Such high loads caused residual stresses, and was responsible for a poor degree of replication in Micro-channels. At 120°C, close to glass transition zone, the replication accuracy was decreasing as the load increased because of less recovery of the polymer chains. Percentage of replication accuracy changed depending upon the size of the features irrespective of the change in parameters. Therefore Macro and Micro-features should be embossed independently with suitable parameters.

Acknowledgement

This work was performed in part at the Melbourne Centre for Nanofabrication (MCN) in the Victorian Node of the Australian National Fabrication Facility (ANFF)

References

- [1] H. Becker and C. Gärtner, "Polymer microfabrication technologies for microfluidic systems," *Analytical and Bioanalytical Chemistry*, 390, 89–111, 2008.
- [2] G. Cheng, M. Sahli, J. Gelin, and T. Barriere, "Journal of Materials Processing Technology Physical modelling, numerical simulation and experimental investigation of microfluidic devices with amorphous thermoplastic polymers using a hot embossing process," *Journal of Materials Processing Technology*, 229, 36–53, 2016.
- [3] S. Tripathi, Y. V. B. Kumar, A. Agrawal, A. Prabhakar, and S. S. Joshi, "Microdevice for plasma separation from whole human blood using bio-physical and geometrical effects," *Scientific Reports*, 6, 26749, 2016.

- [4] D. Sugumar, A. Ismail, M. Ravichandran, I. Aziah, and L. X. Kong, "Amplification of SPPS150 and Salmonella typhi DNA with a high throughput oscillating flow polymerase chain reaction device," *Biomicrofluidics*, 4, 024103, 2010.
- [5] H. Chen *et al.*, "Highly-sensitive capture of circulating tumor cells using micro-ellipse filters," *Scientific Reports*, 7, 610, 2017.
- [6] D. Di Carlo, J. F. Edd, D. Irimia, R. G. Tompkins, and M. Toner, "Equilibrium separation and filtration of particles using differential inertial focusing," *Analytical Chemistry*, 80, 2204–2211, 2008.
- [7] P. Sajeesh and A. K. Sen, "Particle separation and sorting in microfluidic devices: A review," *Microfluidics and Nanofluidics*, 17, 1–52, 2014.
- [8] J. Zhang, S. Yan, R. Sluyter, W. Li, G. Alici, and N.-T. Nguyen, "Inertial particle separation by differential equilibrium positions in a symmetrical serpentine micro-channel," *Scientific Reports*, 4, 4527, 2014.
- [9] T. Jagadesh and G. L. Samuel, "Mechanistic and Finite Element Model for Prediction of Cutting Forces during Micro-Turning of Titanium Alloy," *Machining Science and Technology*, 19, 593–629, 2015.
- [10] R. K. Jena, C. Y. Yue, and Y. C. Lam, "Micro fabrication of cyclic olefin copolymer (COC) based microfluidic devices," *Microsystem Technologies*, 18, 59–166, 2012.
- [11] A. G. G. Toh, Z. F. Wang, and Z. P. Wang, "Ambient hot embossing of polycarbonate, poly-methyl methacrylate and cyclic olefin copolymer for microfluidic applications," *2009 Symposium on Design, Test, Integratio & Packaging of MEMS/MOEMS*, 1–4, 2009.
- [12] R. Suriano *et al.*, "Femtosecond laser ablation of polymeric substrates for the fabrication of microfluidic channels," *Applied Surface Science*, 257, 6243–6250, 2011.
- [13] U. M. Attia, S. Marson, and J. R. Alcock, "Micro-injection moulding of polymer microfluidic devices," *Microfluidics and Nanofluidics*, 7, 1–28, 2009.
- [14] H. Wang, Y. Liu, C. Liu, J. Huang, P. Yang, and B. Liu, "Microfluidic chip-based aptasensor for amplified electrochemical detection of human thrombin," *Electrochemistry communications*, 12, 258–261, 2010.